MCN
Molecular and Cellular
Neuroscience

ELSEVIER

Available online at
ScienceDirect
www.sciencedirect.com

Receptor tyrosine phosphatases regulate birth order-dependent axonal fasciculation and midline repulsion during development of the *Drosophila* mushroom body

Mitsuhiko Kurusu[a,b,*] and Kai Zinn[a,*]

[a]*Broad Center, Division of Biology, California Institute of Technology, Pasadena, CA 91125 USA*
[b]*Structural Biology Center, National Institute of Genetics, and Department of Genetics, The Graduate University for Advanced Studies, Mishima 411-8540, Japan*

Receptor tyrosine phosphatases (RPTPs) are required for axon guidance during embryonic development in *Drosophila*. Here we examine the roles of four RPTPs during development of the larval mushroom body (MB). MB neurons extend axons into parallel tracts known as the peduncle and lobes. The temporal order of neuronal birth is reflected in the organization of axons within these tracts. Axons of the youngest neurons, known as core fibers, extend within a single bundle at the center, while those of older neurons fill the outer layers. RPTPs are selectively expressed on the core fibers of the MB. Ptp10D and Ptp69D regulate segregation of the young axons into a single core bundle. Ptp69D signaling is required for axonal extension beyond the peduncle. Lar and Ptp69D are necessary for the axonal branching decisions that create the lobes. Avoidance of the brain midline by extending medial lobe axons involves signaling through Lar.

Introduction

The mushroom bodies (MBs) are highly conserved paired structures in the insect brain that are essential for olfactory learning and other higher-order functions. MBs vary greatly in size between insect species, but their overall organization is very similar in all insects (for review see (Fahrbach, 2006; Heisenberg, 2003; Strausfeld et al., 1998)). In *Drosophila*, an adult MB contains about 2500 principal neurons, known as Kenyon cells. All Kenyon cells are generated from four neuroblasts (NBs) in each brain hemisphere. Each NB produces three types of Kenyon cells (γ, α′/β′, and α/β) in a strict temporal order, and the four lineages are indistinguishable. An MB is thus a fourfold-symmetric structure (Ito et al., 1997). γ neurons are generated by the mid-third instar stage, α′/β′ neurons between mid-third instar and puparium formation, and α/β neurons after puparium formation.

Kenyon cell dendrites extend into a glomerular structure called the calyx, which receives olfactory input from the projection neurons of the antennal lobe (AL). The axons of Kenyon cells from each lineage group fasciculate into a bundle, and the four bundles merge to form the peduncle, a massive parallel tract that extends ventrally and then splits into two branches, each composed of intertwined lobes.

The three types of Kenyon cells differ with respect to their dendritic and axonal projection patterns in the calyx and lobes (Crittenden et al., 1998; Lee et al., 1999; Strausfeld et al., 2003; Zhu et al., 2003). γ, α′/β′, and α/β neurons receive projections from different sets of AL glomeruli (Lin et al., 2007; Masuda-Nakagawa et al., 2005) and have different roles in memory formation (Pascual and Preat, 2001; Zars et al., 2000).

In larvae, the axonal structures formed by the splitting of the peduncle are called the dorsal and medial lobes. Every Kenyon cell axon bifurcates during outgrowth and sends a branch into each lobe. The γ axons extend first and may serve as pathways to guide the axons of later-born α′/β′ neurons in the larva. αβ neurons follow similar trajectories during the pupal phase. The distal portions of the γ axons degenerate during pupal development, and their medial branches later regrow to form the adult γ lobe. The adult MB has a dorsal branch composed of the intertwined α and α′ lobes, and a medial branch containing the β, β′, and γ lobes (Crittenden et al., 1998). The lobes within the medial branch extend toward the corresponding lobes of the MB in the other hemisphere, but stop at the edge of a midline region that is devoid of MB axons.

The temporal order of Kenyon cell birth is reflected in the organization of axons in the peduncle and lobes, with the axons of the youngest neurons (the core fibers) in the center and those of older neurons arranged as a series of concentric rings around the core

(Kurusu et al., 2002). The core fibers and the layers formed by older axons can be distinguished using antibody markers, GAL4 drivers, and staining for polymerized actin using phalloidin. The actin-rich core fibers are a transient population, because the ingrowth of new axons from sequentially generated later-born neurons occurs successively at the center and displaces the old core fibers outward into the innermost ring. Axons lose bright phalloidin staining as they move outward within the peduncle. This organization is consistent with the idea that the core fibers form a pioneer pathway used to

guide extension of the axons of later-born neurons, which then in turn become the new core and are used as pathways by still later axons(Kurusu et al., 2002). To understand axon guidance and lobe morphogenesis during MB development, it is thus valuable to define and genetically characterize receptors and adhesion molecules expressed on these core fibers.

In this paper, we show that four receptor tyrosine phosphatases (RPTPs) are selectively expressed on core fibers within the peduncle and lobes, and that RPTP signaling regulates segregation of core
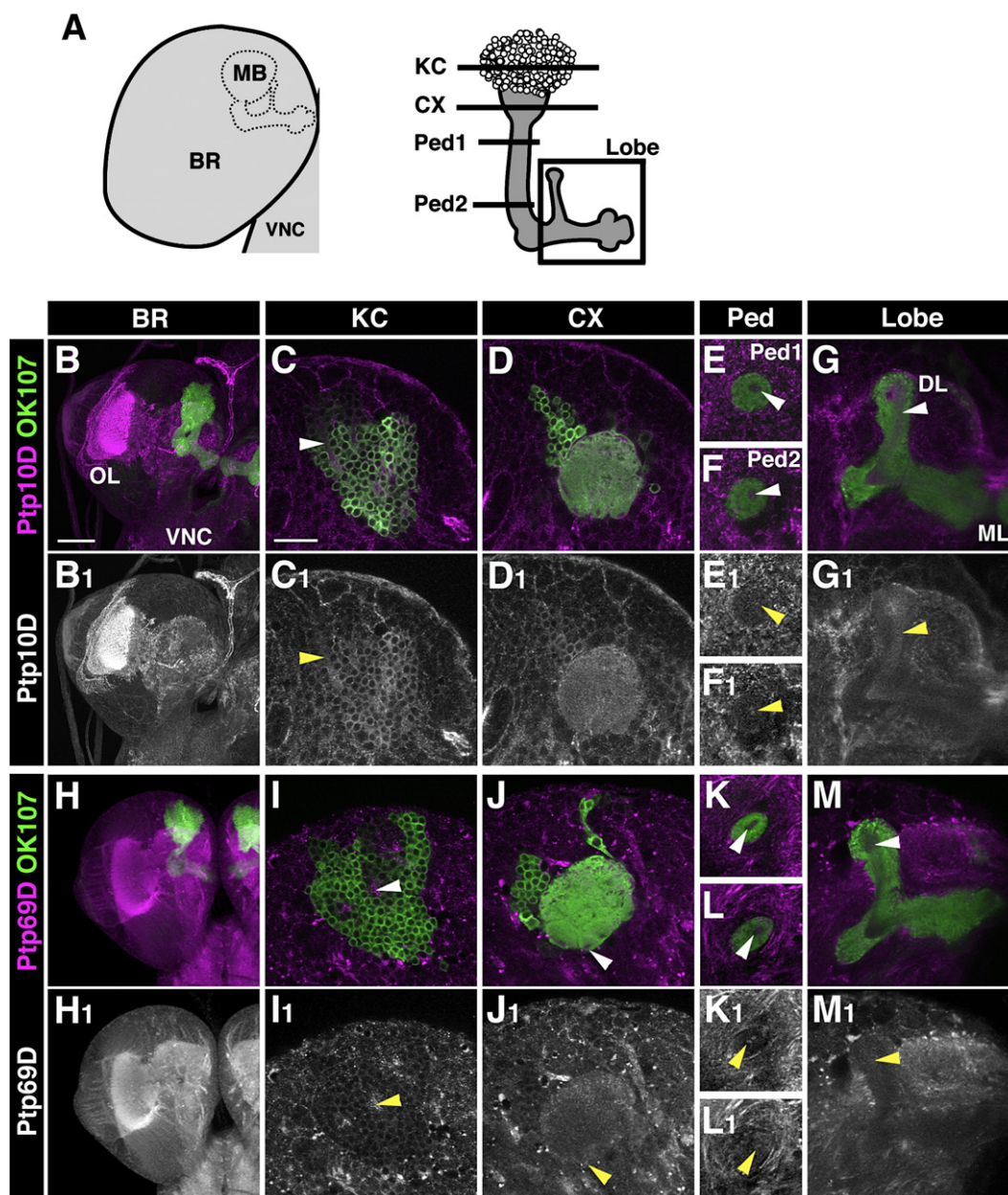
Fig. 1. RPTPs are selectively expressed on young axons in the third instar larval MB. Brains from OK107-GAL4, UAS-mCD8-GFP larvae were stained with mAbs against RPTPs (magenta and white) and visualized using confocal microscopy. The GFP signal is green. In each pair of panels (e.g. B and B1), the first (color) shows both signals, and the second (black and white) shows only the RPTP signal. (B, H, N, and T) Reconstructions of optical sections. The remainder of the panels show single optical sections, with their positions indicated by planes through the MB diagram in (A). In each panel, the arrowheads indicate regions showing selective expression of the RPTP. See text for interpretation. (A) Schematic representations of brain and MB. (B–G and B1–G1) Ptp10D expression. (H–M and H1–M1) Ptp69D expression. (N–S and N1–S1) Ptp99A expression. (T–Y and T1–Y1) Lar expression. (F2, K2, R2, and X2) Higher magnification views of the F, F1, K, K1, R, R1, X, and X1 panels. Abbreviations: BR, brain; OL, optic lobe; MB, mushroom body; VNC, ventral nerve cord; KC, Kenyon cell body clusters; CX, calyx; Ped, peduncle; DL, dorsal lobe; ML, medial lobe. Bar in (B), 50 μm: applies also to (H, N, and T); bar in (C), 20 μm: applies also to (C–G, I–M, O–S, and U–Y).

Author's personal copy

M. Kurusu, K. Zinn / Mol. Cell. Neurosci. 38 (2008) 53–65   55
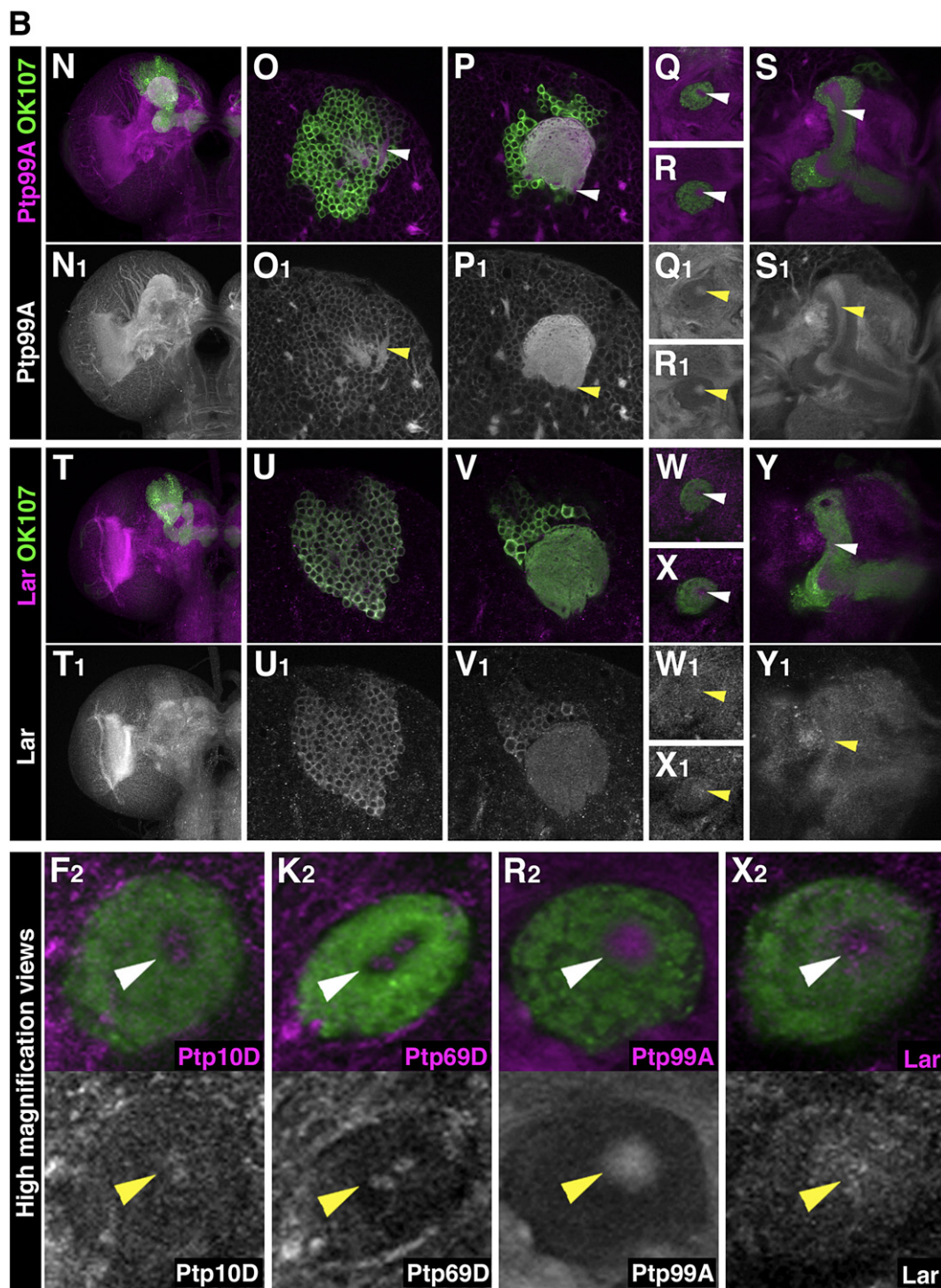
Fig. 1 (*continued*).

fibers into a single bundle. RPTPs have cellular adhesion molecule (CAM)-like extracellular regions containing immunoglobulin (Ig) domains and/or fibronectin type III (FN3) repeats (for review see (Johnson and Van Vactor, 2003)). The ligands that interact with these extracellular domains are largely unknown. However, vertebrate and *Drosophila* Lar RPTPs bind to heparan sulfate proteoglycans (HSPGs), and the cell-surface HSPG Syndecan (Sdc) contributes to Lar's functions during axon guidance and synaptogenesis (Aricescu et al., 2002; Fox and Zinn, 2005; Johnson et al., 2006).

The four RPTPs we localized to core fibers are Lar, Ptp10D, Ptp69D, and Ptp99A. They are all selectively expressed on central nervous system (CNS) axons in the embryo (Desai et al., 1994; Tian et al., 1991; Yang et al., 1991). There are a total of six RPTPs encoded in the *Drosophila* genome. We did not study the other two RPTPs, Ptp52F and Ptp4E, because *Ptp52F* mutants die as embryos (Schindelholz et al., 2001) and *Ptp4E* mutants have not been characterized. Also, good antibodies against these two proteins are not available.

RPTPs have been extensively analyzed as regulators of motor axon guidance in the embryonic neuromuscular system. Each guidance decision made by motor axons can be defined by a requirement for a specific subset of the five RPTPs that have been examined. There is substantial redundancy among RPTPs, so that high-penetrance alterations in a guidance decision are usually observed only when two or more RPTPs are removed. For example, axons of the ISNb nerve fail to leave the common ISN pathway and thus remain fasciculated to ISN axons ('fusion bypass' phenotype) when Lar, Ptp69D, and Ptp99A are all absent (Desai et al., 1997). When only Lar is missing, ISNb axons leave the ISN but then sometimes fail to enter their target muscle field ('parallel bypass' phenotype) (Desai et al., 1997; Krueger et al., 1996).

RPTPs also regulate CNS axon guidance in a redundant manner. A subset of longitudinal axons abnormally cross the midline in *Ptp10D Ptp69D* double mutants (Sun et al., 2000), while all longitudinal axons are rerouted into midline-crossing commissural pathways in *Lar Ptp10D Ptp69D Ptp99A* quadruple mutants (Sun et al., 2001). All four RPTPs thus participate in midline-crossing decisions in the embryo. In this paper, we show that Lar regulates avoidance of the brain midline by MB axons in the larval brain, and that high-penetrance ectopic crossing phenotypes are observed when only Lar is absent.

RPTP function has also been characterized during later development and in adulthood. *Lar* mutants have reduced numbers of boutons at neuromuscular junctions (NMJs) in larvae (Kaufmann et al., 2002), and *Lar* and *Ptp69D* mutants display alterations in photoreceptor axon guidance and synaptic maintenance in the optic lobes (Clandinin et al., 2001; Garrity et al., 1999; Maurel-Zaffran et al., 2001; Newsome et al., 2000). Finally, hypomorphic *Ptp10D* mutants are defective in long-term memory formation, and this phenotype can be rescued by restoration of Ptp10D expression in the MB or by acute induction of Ptp10D in adults (Qian et al., 2007). This result indicates that RPTPs are likely to regulate synaptic function in mature animals. Consistent with this, we show here that all four RPTPs are expressed in specific patterns within the neuropil of the adult brain.

Results

RPTPs are selectively expressed on young axons in the mushroom body

To define the expression patterns of Lar, Ptp10D, Ptp69D, and Ptp99A in the larval and adult MBs, we first examined monoclonal antibodies (mAbs) against the four proteins for their ability to stain larval brain/ventral nerve cord preparations. The original mAbs against Ptp10D, Ptp69D, and Ptp99A were generated against extracellular domain fusion proteins (probably non-native) made in *E. coli* (Desai et al., 1994; Tian et al., 1991). The mAbs against Ptp10D and Ptp99A worked well for staining methanol-fixed whole-mount embryos and for Western blotting, but did not work for immunoprecipitation. mAbs against Ptp69D, however, worked for all three applications. Subsequently, the Zinn group generated mAbs against native Ptp10D, Ptp99A, and Lar extracellular domain fusion proteins made in monkey COS7 cells (Sun et al., 2000) (and unpublished). These mAbs worked for immunoprecipitation but not for Western blotting. When we tested all these mAbs for staining of larval and adult preparations (not methanol-treated), we observed that mAbs against *E. coli*-derived Ptp10D and Ptp99A did not stain, or stained very poorly, while mAbs

against the native proteins (8B2 and 4C7 shown in Supp. Fig. 1) brightly stained the neuropil regions of the brain and ventral nerve cord (compare to phalloidin staining pattern, panel A; phalloidin binds to polymerized actin). mAbs against Ptp69D and Lar stained similar patterns (Supp. Fig. 1). This has been our general observation for many antigens; to obtain good staining of larval preparations with mAbs it is usually necessary to make them against native proteins. Ptp69D is an exception to this rule, since the mAbs against *E. coli* protein worked well for larval staining.

We then examined expression of the four RPTPs in the larval MB and elsewhere in the brain using confocal microscopy. The diagram in Fig. 1A depicts the regions shown in the various panels, indicated by planes through the MB cartoon. These are: the Kenyon cell body region (KC), the calyx (CX) (containing the dendrites of the Kenyon cells and the axon bundles from the four NB lineages that converge to form the peduncle), two sections through the peduncle (the tract containing the Kenyon cell axons), and a section (perpendicular to the other planes) through the lobe regions. Panels 1B–1Y show staining with the anti-Ptp mAb (magenta) together with mCD8-GFP driven by the MB-specific OK107 GAL4 driver. Panels 1B1–1Y1 show the anti-Ptp mAb signal alone, in white.

The data show that each RPTP is expressed in a distinct pattern. All four are expressed in the optic lobes (OL) and elsewhere in the brain neuropil; Ptp10D (B, B1) and Lar (T, T1) are selectively enriched in the optic lobes, while the others are expressed at similar levels in the optic lobes and elsewhere. Ptp10D can be detected on the Kenyon cell bodies (C, C1), but staining is much brighter in the calyx region (D, D1). The four axon bundles that converge to form the peduncle can also be visualized at the bottom of the calyx, and the core fibers can be seen as dark spots within these bundles, since they express GFP only at low levels (one of these is indicated by an arrowhead in J).

Within the peduncle, some or all of the core fibers at the center, which correspond to the axons from the youngest neurons, stain with the anti-Ptp10D mAb, and the entire core fiber bundle expresses GFP at low levels relative to the surrounding axons. As a consequence, Ptp10D staining appears as a small white spot in (F1) (arrowhead), and a larger magenta spot is seen in (F). A high-magnification view of this peduncle section is shown in (F2). Ptp10D is not expressed, or is present at lower levels, on the older axons in the peduncle. Within the dorsal (DL; white arrowhead) and medial (ML) lobes, the axons of young neurons can be visualized as the interior magenta regions (G); these axons (yellow arrowhead in G1) express Ptp10D while the older axons around them do not.

Ptp69D shows less expression in the Kenyon cell body region and calyx than does Ptp10D; however, there are localized areas within the cell body region that have high expression levels (arrowhead in I1). Ptp69D is expressed at higher levels on the core fiber bundles exiting the calyx (arrowhead in J1). Like Ptp10D, it is localized to core fibers within the peduncle (arrowheads in K1, L1; high-magnification views in K2). Expression on the young axons of the lobes is less prominent than for Ptp10D, but the core regions of the lobes (arrowhead in M1) still stain more brightly than the surrounding regions.

Ptp99A is expressed at high levels throughout the calyx (P, P1), and within distinct areas of the Kenyon cell body region (arrowhead in O1). It is also selectively expressed on the core fibers of the peduncle (arrowheads in Q1, R1; high-magnification views in R2). Note that the diameter of the core region expressing Ptp99A is larger than that of the regions expressing Ptp10D and Ptp69D. This suggests that Ptp10D and Ptp69D might be restricted to the youngest

axons, while Ptp99A continues to be expressed on somewhat older axons that are at a greater distance from the center of the core. Within the lobes, Ptp99A is expressed at very high levels in the core region (arrowhead in S1).

Like Ptp10D, Lar is uniformly expressed in the Kenyon cell bodies and calyx (U,U1,V,andV1); however, the relative intensity of staining of these two areas is reversed, with Lar staining being brighter on the cell bodies and Ptp10D staining being brighter in the calyx. In the peduncle, its expression resembles that of Ptp99A, as staining for Lar is observed in an expanded core region. However, the difference in staining intensity between the core and outer layers is less pronounced for Lar than for Ptp99A, with the result that the core fibers are less obvious in anti-Lar stained preparations (arrowheads in W1, X1; high-magnification views in X2). Finally, Lar staining within the lobes is similar to that for the other RPTPs. It is expressed at higher levels on the younger axons in the core (arrowhead in Y1).

In summary, while each of the four RPTPs has a distinct expression pattern in the larval MB, they all are selectively expressed on young axons within the core of the peduncle and lobes. The peduncle section images (F2, K2, R2, and X2) suggest that Ptp10D and Ptp69D might be restricted to the youngest axons, while Ptp99A and Lar continue to be expressed on somewhat older axons that surround the innermost core.

We also examined expression of each RPTP in the adult brain. This analysis (Fig. 2) revealed that Ptp69D, Ptp99A, and Lar are widely expressed in the brain neuropil. Ptp10D has a more selective expression pattern, being present at high levels in the ALs (arrowhead in A1) and MB (B1, C1), and at lower levels elsewhere in the neuropil. Adult Ptp10D expression was also examined by (Qian et al., 2007). Ptp99A is widely expressed in the brain, including the MB, and the MB outline can be detected in the Ptp99A-alone images (H1, L1). Interestingly, Ptp99A is present at especially high levels on the medial lobes (arrowhead in H1). Lar is prominent in the MB, and its levels are somewhat higher in the medial lobes (K, K1, L, and L1). It is also widely expressed elsewhere in the brain (J1). Ptp69D does not show any selective expression in the MB (the MB outline is not visible in E1 or F1).

Ptp10D mutants display core fiber segregation phenotypes

Fig. 3 shows the phenotypes produced by mutations in the two RPTP genes that are not required for viability, *Ptp10D* and *Ptp99A*. In these experiments, third instar larval and adult MB fibers were visualized with the 1D4 mAb against the cytoplasmic domain of Fasciclin II (FasII) (Vactor et al., 1993) using confocal microscopy. Reconstructions of optical sections are shown in panels A–F and N–P.

Ptp10D[1] mutants have very weak MB phenotypes, in which about 3% of MBs display a branching defect. Panel C shows an MB in the larval brain where the dorsal lobe is thin (open arrowhead). The *Ptp10D[1]* mutation is an imprecise excision derivative of a P element located just upstream of the transcribed region. It removes the first exon, containing the signal sequence, and Ptp10D protein is almost undetectable in *Ptp10D[1]* mutant embryos (Sun et al., 2000). Nevertheless, the mutation is probably not a null, as cryptic signal sequences within the large intron downstream of the excised sequence could be joined to the remainder of the protein in order to allow some synthesis of Ptp10D protein.

We also examined larvae and adults hemizygous for Δ59, a deletion that removes all of Ptp10D. This has more severe embryonic phenotypes than *Ptp10D[1]* in some genetic contexts (unpublished).
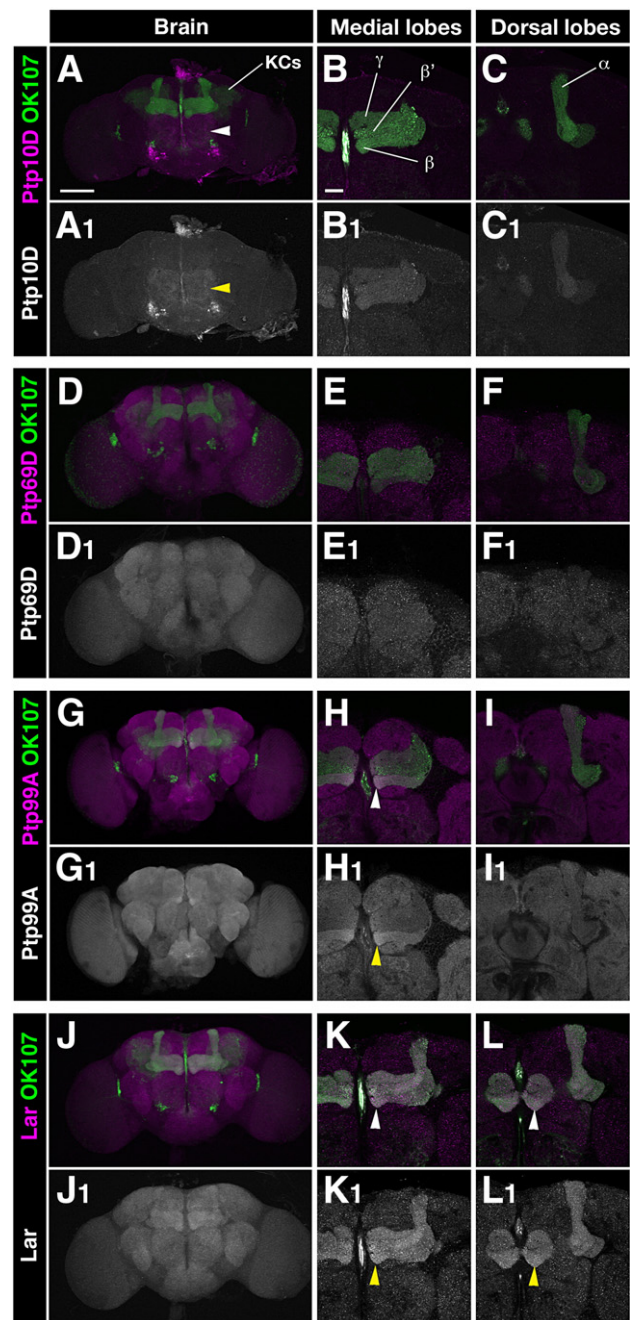

Fig. 2. RPTPs are expressed in the neuropil of the adult brain. Brains from OK107::mCD8-GFP animals are shown, stained with anti-RPTP (magenta/ white) as in Fig. 1. (A, A1, D, D1, G, G1, J, and J1) Reconstructions of optical sections. The rest of the panels show single optical sections, focusing on MB medial lobes (B, B1, E, E1, H, H1, K, and K1) and dorsal lobes (C, C1, F, F1, I, I1, L and L1). In each pair of panels, the upper (color) shows both the anti-RPTP and GFP signals, so that the MB is labeled in green, while the lower (black and white) shows only the anti-RPTP signal. (A–C and A1–C1) Ptp10D expression. Note that the ALs (arrowhead) are much brighter than the rest of the brain. The MB lobes are prominent in (B1) and (C1). (D–F and D1–F1) Ptp69D expression. (G–I and G1–I1) Ptp99A expression. All neuropils are stained brightly by anti-Ptp99A. Note that the medial lobes of the MBs are brighter than the surrounding structures (arrowheads). (J–L and J1–L1) Lar expression. The MB medial lobes are also prominent (arrowheads). Bar in (A), 50 μm: applies also to (D, G, and J); bar in (B), 20 μm: applies also to (C, E–F, H–I, and K–L).

Δ59 animals have much stronger MB phenotypes; only 40% of MBs are normal, and 10% display branching defects (panel 3B, open arrowhead) like those in panel 3C. Two other types of defects are also observed. In 30% of larvae, the medial lobe of one or both of the MBs extends past its normal termination point and crosses the midline of the brain, leading to an apparent fusion of the medial lobes (ML fusion, panel 3B, arrowhead). [Note that in scoring ML fusion, we cannot determine if it arises from overextension of one or both MBs in a larva. Thus, our observation of ML fusion in 30% of the larvae we examined indicates that 15–30% of MBs have lobes that abnormally extend across the midline.]

In 25% of Δ59 MBs, examination of single optical sections through the peduncle reveals defects in the organization of the core fibers. Panel 3G shows a control section with a normal morphology, in which a small core fiber region, labeled with phalloidin (magenta), is surrounded by older axons, labeled with anti-FasII (green). In panel H, a Δ59 section with a core defect is shown. In this section, the core fibers are split into three distinct bundles
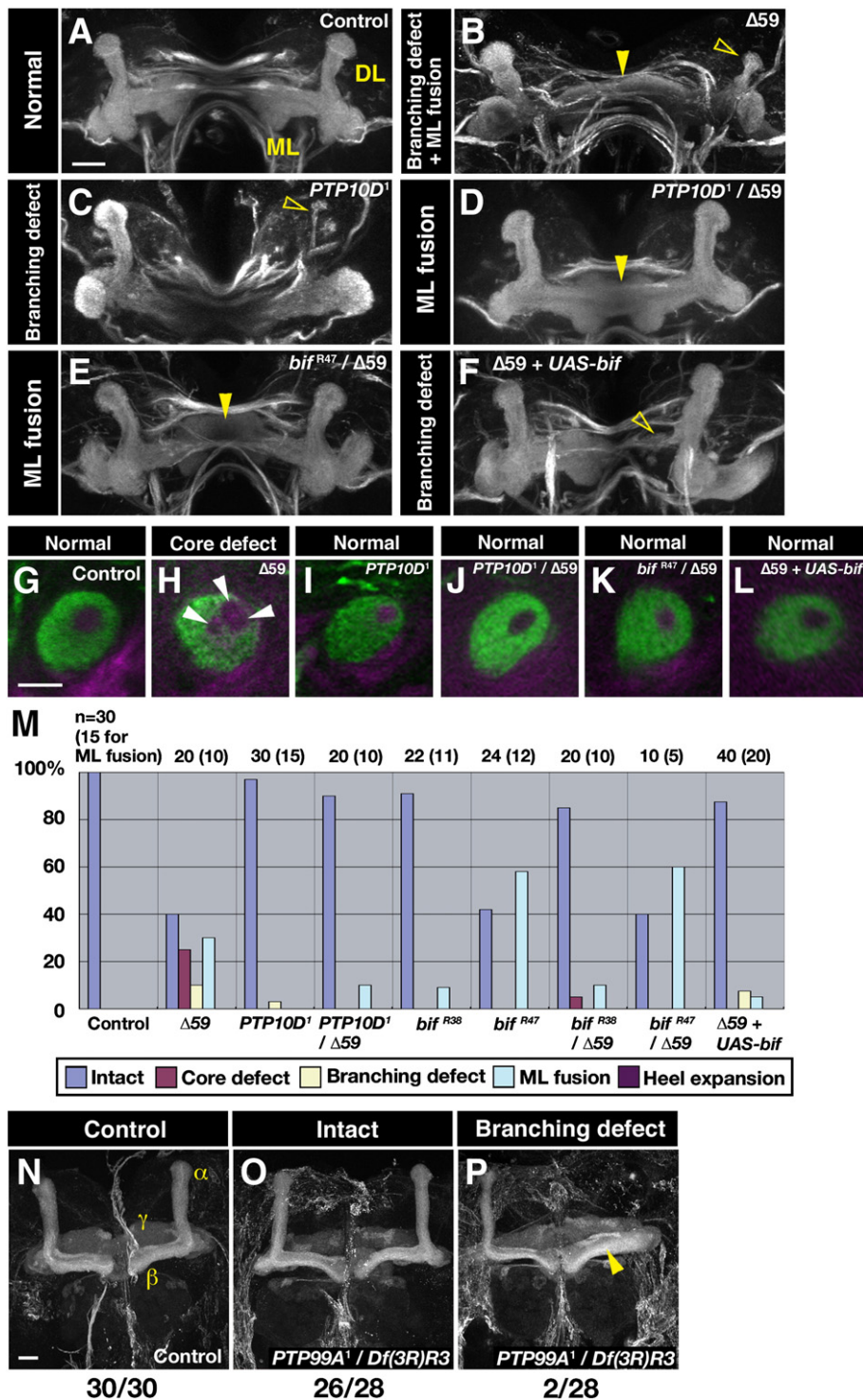
(arrowheads) and these core bundles occupy a larger region of the peduncle than in normal MBs.

Δ59 also removes the gene 3′ to *Ptp10D*, *bifocal* (*bif*) (Bahri et al., 1997). Bif is an actin-binding protein that is associated with the serine-threonine phosphatase PP1(Babu et al., 2005, 2004). Bif also associates with and is a substrate for the serine-threonine kinase Misshapen (Ruan et al., 2002). In *bif* mutants, R1-6 photoreceptor axons sometimes bypass their normal targets in the lamina(Babu et al., 2005; Ruan et al., 2002). To investigate whether loss of Bif contributes to the *Δ59* MB phenotype, we examined hemizygotes for two *bif* alleles, *bif*[R47] and *bif*[R38], and also combined *Δ59* with a UAS–Bif construct and the OK107 GAL4 driver.

Our results show that MB axon guidance has a complex dependence on Bif that differs for each of the three phenotypes examined. Branching defects are not seen in *bif* mutants, and are not affected by driving Bif in the *Δ59* background (Fig. 3M). These, therefore, are due entirely to loss of Ptp10D. Neither of the *bif* mutants have core fiber defects, and they are also not seen in *Ptp10D*[1] animals (Fig. 3I–K). However, UAS–Bif eliminates the core fiber defects seen in *Δ59* mutants (Fig. 3L, M). Core fiber segregation defects are thus produced only when both Ptp10D and Bif are absent. *Ptp10D* and *bif* were already shown to interact genetically in producing R1-6 photoreceptor axon guidance phenotypes (Babu et al., 2005). This is interesting, since it implies that these two adjacent genes have a selective genetic interaction. Finally, the ML fusion defect is attributable exclusively to loss of Bif, as *bif*[R47] mutants display this defect with a penetrance higher than that seen for *Δ59* (Fig. 3E, M), and the *Δ59* ML fusion phenotype is almost eliminated by driving UAS–Bif in the MB (Fig. 3F, M). The *bif*[R47] phenotype is stronger than that of *bif*[R38]; this was also observed by (Ruan et al., 2002).

Ptp99A null larvae (genotype *Ptp99A*[1]*/Df(3R)R3*) (Hamilton et al., 1995) did not display MB phenotypes, and the overall structure of the brain was also normal (data not shown). Two of 28 adult MBs examined, however, had branching defects in which the α lobe was missing and the β lobe was enlarged (Fig. 3P). This phenotype suggests that the α lobe axons were rerouted into the β lobe.

Ptp69D signaling affects segregation of core fibers

Ptp69D null mutants (transheterozygotes for *Ptp69D*[1]*/Df(3L) 8ex25*) (Desai et al., 1996) usually die as early larvae, but some survive until third instar. These mutants were previously shown to have defects in photoreceptor axon guidance (Garrity et al., 1999). We examined the brains of *Ptp69D* null larvae, and found that all structures are disrupted. *Ptp69D* mutants have organized anti-FasII

stained optic lobe structures (compare Fig. 4, panels A1 and C1), but their MBs are unrecognizable (arrowheads in panels C1 and D). The entire phalloidin-stained actin network of the brain is chaotic (panel C2). This makes it impossible to evaluate specific roles for Ptp69D in MB development using these larvae.

Because of these considerations, we examined the consequences of selective MB expression of a dominant-negative Ptp69D construct, Ptp69D[DA3]. This is a mutant that bears aspartate (D)-to-alanine (A) substitutions in the active sites of both of its tandem PTP domains (Garrity et al., 1999). These D-to-A mutants act as 'substrate traps', in that they bind to tyrosine-phosphorylated substrates but do not catalyze dephosphorylation. Their ability to act as traps is due to the absence of the aspartate residue, which normally donates a proton to the phosphorus–oxygen bond, allowing it to be successfully attacked by the thiol nucleophile of the essential cysteine residue (Flint et al., 1997). Previous work by our group has shown that expression of the Ptp69D[DA3]construct in embryonic neurons (unpublished) generates motor axon guidance phenotypes like those produced by *Ptp69D* LOF mutations (Desai et al., 1996; Desai et al., 1997). These may arise from sequestration of Ptp69D substrates.

We expressed Ptp69D[DA3] using two different MB drivers: OK107-GAL4, which is expressed in all differentiated Kenyon cells, and 201Y-GAL4, which is expressed only in older Kenyon cells that have already extended axons. The distinction between the timing of OK107 and 201Y-driven expression can be seen by examination of sections through the peduncle; the core fibers express OK107-driven GFP weakly, but all surrounding axons express it at high levels (see Fig. 1). 201Y, in contrast, is not expressed at all in the core, and exhibits strong expression only in the outer layers containing older axons (Kurusu et al., 2002). We observed phenotypes only when Ptp69D[DA3] was expressed using OK107 (Fig. 4E–I, N). All MBs expressing the construct from 201Y were normal (Fig. 4J–N). These data suggest that Ptp69D functions primarily during the period of axon extension.

Expression of Ptp69D[DA3] using OK107 generated very strong phenotypes. In almost all MBs (>90%), the 'heel' region of the MB (at or near the junction of the peduncle and lobes) was expanded at the expense of the dorsal and medial lobes (Fig. 4F (arrowhead), N). These phenotypes suggest that axons normally destined for the dorsal and/or medial lobes stop in the heel region when Ptp69D substrates are sequestered. In 57% of MBs, one of the residual lobes was much larger than the other (Fig. 4G), suggesting that one branch stayed in the heel region while the other entered the lobe. These phenotypes likely involve a general defect in axon outgrowth, since the axons that expand the heel are stopping at the distal end of the peduncle and failing to extend into the lobes.

Fig. 3. Core splitting and branching defects in *Ptp10D* mutants. Third instar larval brains (A–F) and adult brains (N–P), showing morphologies of MB lobes visualized with anti-Fas II. Reconstructions of optical sections are shown. (A) Wild-type control. (B) ML fusion and branching defect, in a *Δ59* hemizygote. The MLs from the two hemispheres are fused at the midline (arrowhead). The dorsal lobe in the right hemisphere is very thin (open arrowhead). (C) A Ptp10D[1] MB with a branching defect, showing a thin dorsal lobe in the right hemisphere (open arrowhead). (D) MB from a *Ptp10D*[1]*/Δ59* transheterozygote, showing an ML fusion (arrowhead). (E) *bif*[R47]*/Δ59*, also showing ML fusion (arrowhead). (F) *Δ59* with UAS–Bif driven by OK107. The ML is very thin (arrowhead). (G–L) Single optical sections through the peduncle, showing core fiber bundles labeled with phalloidin (magenta) and Fas II expression on surrounding axons (green). (G) Wild-type control. Note the single magenta spot within the green peduncle tract. (H) Core defect, in a *Δ59* MB. Three distinct magenta core fiber bundles are observed (arrowheads). (I–L) Normal peduncles, in four different genotypes. (M) Bar graph showing phenotypic penetrances in *Ptp10D* and *bif* mutants, mutant combinations, and rescued genotypes. Note that the bar height for ML fusion indicates the % of brains affected, while those for other phenotypes indicate the % of MBs affected. (N) Wild-type control brain. The α, β, and γ lobes, which express FasII, are indicated. All wild-type MBs (30/30 brains) had this morphology. (O) 26/28 *Ptp99A*[1]*/Df(3R)R3* brains had normal MB morphologies. (P) 2/28 *Ptp99A*[1]*/Df(3R)R3* brains had an MB with a branching defect in which the α lobe is missing and the β lobe is enlarged. Bar in (A), 20 μm: applies also to (B–F); bar in (G), 10 μm: applies also to (H–L); bar in (N), 20 μm: applies also to (O and P).

We also observed core defects in most MBs expressing Ptp69D^{DA3} from OK107 (~75%) (Fig. 4I, N). These were similar to the split-core phenotypes described above for $\Delta 59$ MBs. In Fig. 4I, four distinct phalloidin-labeled core bundles are observed in a section through the peduncle, and one of these is at the edge of the peduncle rather than in its center. These results indicate that Ptp69D and Ptp10D are important for segregation of core fibers into a distinct bundle.

The phenotypes seen as a consequence of Ptp69D^{DA3} expression in the MB cannot be attributed exclusively to loss of Ptp69D signaling, since substrate sequestration might produce additional phenotypes due to the potential use of these substrates in other pathways. Also, it is unknown whether Ptp69D^{DA3} expression causes a partial or a total loss of Ptp69D function. To further examine these questions, we took three approaches. First, we examined a weak (missense) *Ptp69D* mutant, *Ptp69D^{18}* (Desai and Purdy,
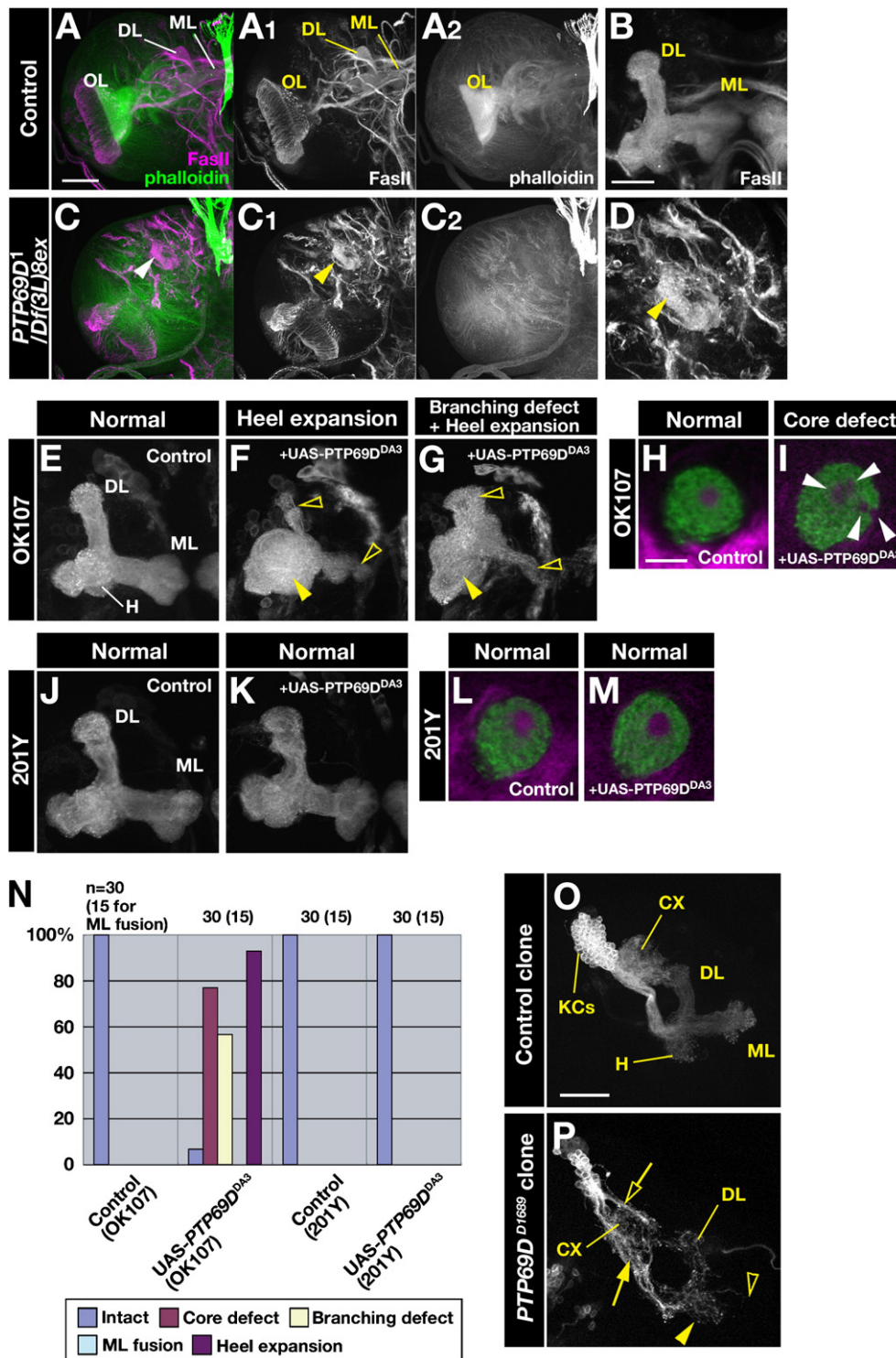
2003). Second, we drove two different Vienna *Drosophila* RNAi Center (VDRC) Ptp69D RNAi lines (Dietzl et al., 2007) in the MB using OK107. Third, we generated MARCM (Lee and Luo, 1999) NB clones of a *Ptp69D* null mutation, *Ptp69D^{D1689}* (Newsome et al., 2000).

We expected that the RNAi and *Ptp69D^{18}* phenotypes would be reflective of a partial loss of Ptp69D function, since RNAi lines normally do not produce null phenotypes. We observed core defects with a very high penetrance (70–100%) for all three genotypes (mutant and the two RNAi lines; Supp. Fig. 2). Branching defects were also seen, with a lower penetrance than that observed for Ptp69D^{DA3}. Oddly, however, the heel expansion defect was not obvious in these lines, but was replaced by a knob-like expansion of a region under the calyx, adjacent to the heel (Supp. Fig. 2). In summary, these results indicate that the axon guidance phenotypes seen in Ptp69D^{DA3} are in fact due to loss of Ptp69D function.

Further evidence for this was provided by the analysis of MARCM NB clones ($n = 8$) for a *Ptp69D* null mutation. A wild-type NB clone (Fig. 4O) induced at the first instar stage and dissected at third instar contains about 200 Kenyon cells, which contribute axons to both the dorsal and medial lobes. *Ptp69D* clones (Fig. 4P) displayed many severe axon guidance defects, including aberrant projections along the iACT pathway taken by antennal lobe axons projecting to the MB (open arrow in (P)), heel expansion (arrowhead), axonal defasciculation (arrow), and loss of the ML (open arrowhead).

Lar regulates repulsion of Kenyon cell axons from the brain midline

Lar mutants typically die during the pupal stage. We examined larval MB phenotypes by staining axons with anti-FasII in three different transheterozygous Lar mutant combinations (*Lar^{5.1}/Lar^{13.2}*, *Lar^{5.5}/Lar^{13.2}*, and *Lar^{OD5}/Lar^{13.2}*) (Krueger et al., 1996), and found that all combinations produced the same phenotypes, with roughly similar penetrances. All of these *Lar* mutations are thought to be nulls. In most animals examined, the dorsal lobes of the MBs were reduced or absent (open arrowheads), and the medial lobes were fused across the midline (closed arrowheads; Fig. 5B–D). 60–100% of brains displayed ML fusion (indicating that the medial lobe axons of 30–100% of the MBs extended across the midline; see note above), while 50–90% of MBs had reduced or missing dorsal lobes (Fig. 5L). Core fiber and heel expansion defects were not observed in *Lar* mutants.

To analyze *Lar* phenotypes in more detail, we used MARCM analysis (Lee and Luo, 1999) to visualize GFP-labeled mutant axons in larval and adult brains. We generated *Lar* NB clones using two point mutations, *Lar^{5.5}* and *Lar^{451}*. Both produced the same phenotypes. In third instar larvae, *Lar* mutant axons extended across the midline and did not stop at their normal termination point (Fig. 5F). This phenotype can be seen in more detail in Fig. 5F1, where GFP-labeled mutant axons are in green and the anti-FasII-labeled scaffold is in magenta (compare to wild-type axons in Fig. 5E1). All wild-type axons stop abruptly near the edge of the midline (ML) region, while some mutant axons extend across the midline and into the contralateral ML (arrowhead, Fig. 5F1). This phenotype was observed in 50% of *Lar^{5.5}* clones and 20% of *Lar^{451}* clones (Fig. 5M). Interestingly, we did not observe branching defects in the larval clones, suggesting that the branching defect (reduction or loss of the dorsal lobe) commonly seen in Lar mutant animals is a property of the whole mutant brain, and may require that all MB axons, and possibly non-MB structures, lack Lar function (Fig. 5M).

Lar mutant clones were also examined in the adult. In a wild-type adult NB clone, there are about 500 neurons, which project into the γ, α′/β′, and α/β lobes in a birth order-dependent manner (Fig. 5G; anti-FasII staining in magenta). About 35% of *Lar^{5.5}* and 25% of *Lar^{451}* clones had β lobe axons that extended across the midline and contacted the axons from the other MB (arrowhead, Fig. 5H, M). Branching defects, in which the size of the β lobe section of the clone was doubled and the vertical (α and α′) lobe sections were missing, were also seen at a low frequency (~8%) in *Lar^{451}* adult clones (Fig. 5I, M). Interestingly, in these cases we did not observe α and α′ lobes that were anti-FasII positive and GFP-negative (these would have arisen from wild-type cells), suggesting that *Lar^{451}* clones can produce a non-autonomous effect on the projections of wild-type axons (Fig. 5I).

Lar mutants have altered neuromuscular junction (NMJ) synapses (Kaufmann et al., 2002), so we were interested in determining whether synapses onto Kenyon cell dendrites would be altered in the absence of Lar function. To do this, we examined single cell/two cell MARCM clones in the adult MB calyx, focusing on γ neurons. In wild-type animals, γ neuron dendrites have claw-like terminals that form the postsynaptic specializations (Fig. 5J, arrowhead). We did not find any systematic alterations in the morphologies of these terminals in *Lar^{5.5}* clones (Fig. 5K).

Finally, we overexpressed all four of the RPTPs in the MB using OK107-GAL4 to drive UAS constructs, to see if forcing

Fig. 4. *Ptp69D* MB phenotypes: core splitting and loss of projections into the lobes. (A–D): third instar larval brain hemispheres stained with anti-FasII (green/white) and phalloidin (magenta/white). (A) and (C) show low-magnification color views of wild-type (A) and *Ptp69D^1/Df(3L)8ex25* (C) brain hemispheres, while panels A1, A2, C1, and C2 show black and white views of separated channels from the same images. (B) and (D) are high-magnification views of the FasII signal from the same brains, showing MB morphology. Reconstructions of optical sections are shown. OL, optic lobe; ML, medial MB lobe; DL, dorsal MB lobe. The arrowheads in (C1) and (D) indicate the MB remnant structure observed in *Ptp69D* brains. Reconstructions of optical sections (E–G, J–K), and single optical sections through the peduncle (H–I, L–M), from OK107::mCD8-GFP larvae (E–I) or 201Y::mCD8–GFP larvae (J–M). (E–G) and (L–K) show the GFP signal, in white, while (H–I) and (L–M) show the GFP signal in green and phalloidin in magenta. (E) Control. The heel region is labeled (H), as are the DL and ML. (F–G) Larvae expressing Ptp69D^{DA3} from OK107. In (F) the heel is expanded (arrowhead) and the DL and ML are thin (open arrowheads). In (G) the heel is expanded and the DL is much larger than the ML, indicating a branching defect. (H) Control peduncle section. Note the single magenta core fiber bundle. (I) Peduncle section from an OK107::Ptp69D^{DA3} larva. The core fibers are split into several distinct bundles (arrowheads). (J) Control MB, showing the 201Y::GFP signal. (K) MB from a 201Y:: Ptp69D^{DA3} larva, showing normal morphology. (L) Control peduncle section. The single core fiber bundle and surrounding older green axons are also seen with 201Y::GFP. (M) Peduncle section from a 201Y::Ptp69D^{DA3} larva, showing a normal core fiber bundle. (N) Bar graph showing phenotypic penetrances in larvae expressing Ptp69D^{DA3}. Bar heights indicate the % of MBs of the indicated genotypes that display the various phenotypes. (O) Control NB MARCM clone. KCs, heel (H), calyx (CX), and dorsal (DL) and medial (ML) lobes are indicated. (P) *Ptp69D^{D1689}* NB clone, displaying severe axon guidance phenotypes. Closed arrowhead, expanded heel; open arrowhead, disappearance of ML; closed arrow, defasciculation of axons beneath calyx; open arrow, ectopic projection of axons into the iACT (the route taken by axons of antennal lobe neurons that project to the calyx). Bar in (A), 50 μm: applies also to (C); bar in (B), 20 μm: applies also to (D, E–G, and J–K); bar in (H), 10 μm: applies also to (I and L–M); bar in (O), 20 μm: applies also to (P).
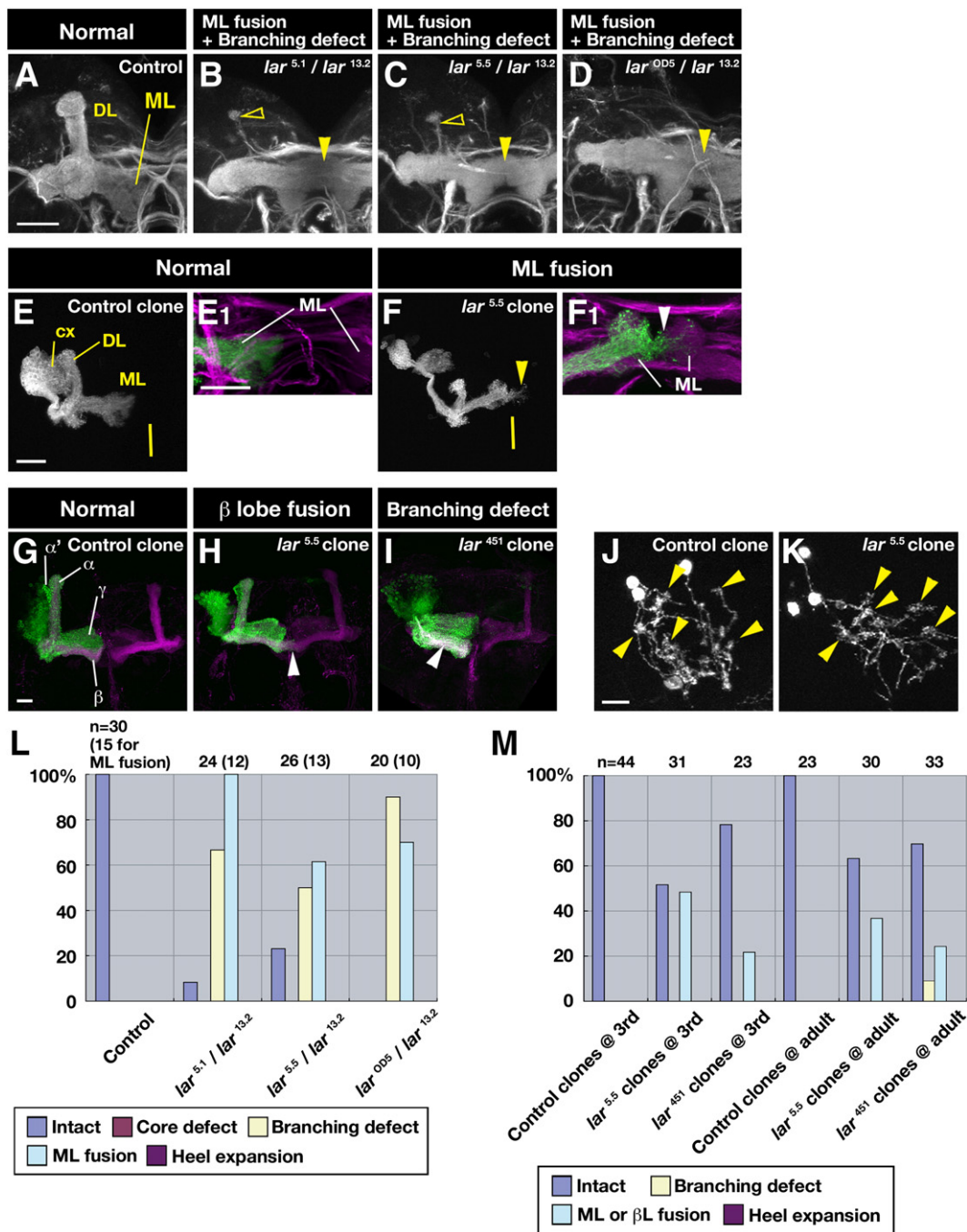
Fig. 5. *Lar* MB phenotypes: medial lobe fusion and branching defects. (A–D) Third instar larval brain hemispheres stained with anti-FasII to reveal MB morphologies. Reconstructions of optical sections are shown. Open arrowheads indicate dorsal lobes (DL); closed arrowheads indicate medial lobes (ML). (A) Wild-type control. (B) *Lar$^{5.1}$/Lar$^{13.2}$* transheterozygote. One DL is thin and the other absent, and the MLs are fused across the midline. (C) *Lar$^{5.5}$/Lar$^{13.2}$* transheterozygote. Same phenotype as in (B). (D) *Lar^{OD5}/Lar$^{13.2}$* transheterozygote. Both DLs are absent and the MLs are fused. (E–I) MARCM NB clones (positively labeled with mCD8-GFP), examined at third instar larval stage (E–F) or in adults (G–I). GFP signal is in green, and anti-FasII in magenta, in (E1) and (F1), which are higher-magnification views; (E) and (F) show the GFP signal alone, in white. The brain midline is indicated by a yellow vertical bar in (E) and (F). (E, E1): control clone, showing the calyx (CX), DL, and ML. Note that the end of the ML portion of the clone is to the left of the brain midline. (F,F1): *Lar$^{5.5}$* clone. Note that the ML axons extend beyond the brain midline (arrowheads), and enter the contralateral ML lobe (arrowhead in F1). (G–I) Adult clones, visualized with mCD8-GFP (green) and anti-FasII (magenta). (G) Control clone. The α, α′, β, and γ lobes are indicated. (H) *Lar$^{5.5}$* clone. Note that some β lobe axons (arrowhead) extend across the brain midline and contact the contralateral anti-FasII-stained β lobe. (I) *Lar^{451}* clone. The α lobe portion of the clone is missing, and the β lobe is doubled in thickness (arrowhead), indicating a defect in branching. (J–K): single cell/two cell MARCM clones, showing dendritic endings in the calyx. The dendrites end in "claw-like" terminals (arrowheads). (J) Control clone. (K) *Lar$^{5.5}$* clone. No obvious difference in morphology of the dendritic endings is seen. (L) Bar graph of phenotypic penetrances in Lar mutant larvae. Note that the bar height for ML fusion indicates the % of brains affected, while those for other phenotypes indicate the % of MBs affected. (M) Bar graph of phenotypic penetrances in *Lar* mutant NB clones examined at the larval or adult stages. Bar in (A), 20 µm: applies also to (B–D); bar in (E), 20 µm: applies also to (F); bar in (E1), 20 µm: applies also to (F1); bar in (G), 20 µm: applies also to (H–I); bar in (J), 10 µm: applies also to (K).

expression of the RPTPs to persist on older axons might alter axon guidance or morphogenesis. We did not observe any phenotypes in these experiments (Supp. Fig. 3).

Discussion

In this paper, we demonstrate that RPTPs are selectively expressed on the core fibers of the MB. At any one time during larval development, the core fiber bundle is composed of the youngest axons within the peduncle and lobes (Kurusu et al., 2002). Core fibers are likely to serve as pathways for guidance of axons of later-born neurons. These later axons then become the new core fiber bundle and displace the old core fibers outward into concentric rings.

Two of the RPTPs, Ptp69D and Ptp10D, are expressed only on the innermost core fibers, while Lar and Ptp99A are expressed within an expanded core region including somewhat older axons (Fig. 1). Our data indicate that Ptp10D and Ptp69D are involved in segregation of core fibers. We observed split-core phenotypes, in which two or more phalloidin-rich, OK107::mCD8-GFP-low bundles are observed within the peduncle, in MBs lacking Ptp69D function (Fig. 4, Supp. Fig. 2). They were also observed in larvae hemizygous for a complete deletion of *Ptp10D* and the adjacent *bif* gene, *Δ59*. The split-core phenotype only occurs when both Ptp10D and Bif are absent (Fig. 3). These two genes have been shown to genetically interact in other contexts (Babu et al., 2005).

Ptp69D is also required for outgrowth of axons from the peduncle into the lobes, because regions near the junctions of the peduncle and the lobes are expanded at the expense of the lobes in MBs lacking Ptp69D function (Fig. 4, Supp. Fig. 2). Another distinctive phenotype seen in our experiments is abnormal extension of medial lobe axons across the brain midline. This is seen in *Lar* mutant larvae and in larval and adult *Lar* mutant NB clones (Fig. 5).

CAMs and CAM-like receptors regulate core fiber segregation

Prior to this work, only two genes had been identified as having mutant phenotypes affecting core fiber segregation. Both of these encode adhesion molecules. mRNA from the Dscam gene, which encodes homophilic Ig domain CAMs, is alternatively spliced to generate up to 38,000 different protein isoforms (Schmucker et al., 2000; Wojtowicz et al., 2004). Like the RPTPs, Dscam is selectively expressed on young axons that travel within the core fiber bundle. Dscam mutant MBs and NB clones exhibited multiple core fiber bundles within the peduncle (Zhan et al., 2004). The similarities between *Dscam*, *Ptp69D*, and *Ptp10D* phenotypes and expression patterns suggest that these RPTPs could be involved in Dscam signaling during outgrowth of young axons within the peduncle. Alternatively, the RPTPs could regulate adhesion via other pathways that also affect core fiber segregation and are partially redundant with Dscam.

Core fiber segregation defects were also observed in ~25% of NB clones bearing null mutations eliminating expression of the homophilic Ig domain CAM FasII. FasII, unlike Dscam and the RPTPs, is only expressed on older axons outside the core region (Kurusu et al., 2002), and engagement between FasII molecules on different cell surfaces is thought to trigger adhesion rather than repulsion. This suggests that core fiber segregation defects in FasII mutants arise by a different mechanism. Perhaps older axons lacking FasII fail to adhere sufficiently to each other and thus open passageways that allow young axons to pioneer multiple pathways within the peduncle.

RPTPs regulate exclusion of MB axons from the midline region of the brain

Mutants lacking expression of Lar exhibit phenotypes in which one or both of the medial lobes of the bilaterally symmetric MBs extend across the midline, so that they appear fused to one another. We also found that *Lar* mutant NB clones extended axons across the midline into the territory occupied by the other MB (Fig. 5). These phenotypes suggest that a repulsive signal emanates from the brain midline region, and that Lar participates in reception of this signal by growing MB axons within the medial lobe.

This is formally similar to repulsion from the CNS midline in the embryo, where binding of midline Slit to Roundabout (Robo) receptors on neuronal growth cones causes them to navigate away from the midline (Kidd et al., 1999). Axons abnormally cross the midline in *Ptp10D Ptp69D* double mutant embryos, and genetic interaction studies showed that these RPTPs are positive regulators of Robo signaling in the embryo (Sun et al., 2000). Lar is also implicated in the decisions of axons to cross the embryonic midline (Sun et al., 2001).

The MB midline-crossing phenotypes seen in *Lar* mutants are probably not mediated through alterations in Slit-Robo signaling. *Robo1*, *2*, and *3* mutant phenotypes in the larval MB have been described, and they do not include fusion of medial lobes across the midline (Nicolas and Preat, 2005). The Lar ligand Sdc is not selectively expressed at the brain midline (unpublished), so binding of Lar to Sdc probably does not trigger repulsion of MB axons. Perhaps other, as yet unidentified, Lar ligands are expressed in the midline region, and interactions between these ligands and the RPTP facilitates repulsion. Studies by our group showed that Lar binds to at least one non-HSPG ligand in the embryo (Fox and Zinn, 2005).

A number of other genes that regulate repulsion of MB axons from the midline have been identified in other studies. Mutations in *derailed (linotte)*, which encodes a protein related to Ryk receptor tyrosine kinases, cause overgrowth of medial lobes across the midline (Moreau-Fauvarque et al., 1998). The Derailed receptor responds to a Wnt5 signal, and mediates exclusion of axons from posterior commissural pathways that cross the embryonic midline (Yoshikawa et al., 2003). Medial lobe fusion across the midline is also observed in *fmr1* mutants and in FMR1 overexpression animals (Michel et al., 2004; McBride et al., 2005; Pan et al., 2004). FMR1 is an RNA-binding protein that is orthologous to the human gene affected in Fragile X mental retardation syndrome.

Other genes potentially involved in repulsion from the brain midline were identified in a microarray screen for MB-expressed genes. ML fusion was observed in some larvae when expression of these genes was inhibited using RNAi methods (Kobayashi et al., 2006). The gene with a known function for which RNAi produced ML fusion with the highest penetrance is CG6083, encoding an aldehyde reductase. RNAi for a gene encoding a cGMP phosphodiesterase also produced ML fusion. cGMP signaling has been implicated in growth cone repulsion in vertebrate neuronal cultures (Nishiyama et al., 2003).

Concluding remarks

The work described in this paper shows that four RPTPs are localized to growing MB axons and are important for the creation of the distinctive architecture of the MB's axonal network. Examination of *Rptp* mutant phenotypes shows that these CAM-like signaling molecules control several different axon guidance

decisions that occur during outgrowth. Ptp10D and Ptp69D regulate segregation of the growing axons into a single core bundle within the peduncle. Ptp69D and Lar are necessary for the later axonal extension and branching events that create the dorsal and medial lobes. Medial lobe axons cease outgrowth before they reach the brain midline, and their decision to stop involves Lar.

Experimental methods

Drosophila stocks

OK107-Gal4, 201Y-Gal4, *piM* FRT40A and UAS-*mCD8*::GFP were obtained from the Bloomington stock center. *Ptp10D[1]* and Δ59 are described in (Sun et al., 2000). *Ptp69D[1]* and *Df(3L)8ex25* are described in (Desai et al., 1996). *Ptp69D[D1689]* is described in (Newsome et al., 2000). *Ptp69D[18]* is described in (Desai and Purdy, 2003). Ptp69D RNAi strains (VDRC#4789 and #27091) were obtained from Vienna *Drosophila* RNAi Center. *Ptp99A[1]* and *Df(3R)R3* are described in (Hamilton et al., 1995). *Lar[5.1]*, *Lar[5.5]*, *Lar[13.2]*, and *Lar[OD5]* are described in (Krueger et al., 1996). *Lar[451]* (Clandinin et al., 2001) was obtained from S.L. Zipursky (UCLA). *bif[R38]* and *bif[R47]* are described in (Bahri et al., 1997). For overexpression analysis, EP1074 (for *Ptp10D*), UAS-*Ptp69D*, UAS-*Ptp69D[DA3]* (Garrity et al., 1999), UAS-*Ptp99A* (B.A. Hamilton and K.Z., unpublished), and UAS-*Lar* (Krueger et al., 1996) were used. For MARCM analyses, hs-*FLP* UAS-*mCD8*::*GFP*; *Gal80* FRT40A; OK107 was provided by L. Luo (Stanford University). C155 UAS-*mCD8*::*GFP* hs-FLP; Gal80 FRT80B was provided by K. Emoto (National Institute of Genetics).

MARCM mosaic analysis

Mosaic clones were generated as described in (Lee and Luo, 1999). Egg collection was done for 2 h window on standard food at 25 °C. A single 60 min heat shock at 37 °C was applied at 27 h after egg collection-starting time for induction of mitotic recombination in the first instar stage. Clones were examined at the wandering larval stage or adult stage.

Immunocytochemistry

The dissected brains were fixed for 30 min with 4% paraformaldehyde at room temperature. Washing was done with 0.3% Triton X-100 in PBS. Blocking was done with 0.3% Triton X-100+0.1% BSA+5% normal goat serum in PBS. Incubation with primary antibody was done overnight at 4 °C. Labeled brains were mounted with anti-fade Vectashield medium (Vector Laboratories, Inc.). Confocal images were captured with an LSM510 instrument. Images were processed using Adobe Photoshop. The following primary antibodies were used: Mouse anti-Ptp10D (clone 8B2) diluted 1:4; mouse anti-Ptp69D (clone 2C2) diluted 1:4; mouse anti-Ptp99A (clone 4C7) diluted 1:4; mouse anti-Lar (clone 9D8) diluted 1:4. Alexa Fluor-conjugated phalloidin was diluted 1:40 (Molecular Probes); mouse anti-FasII (mAb1D4; (Vactor et al., 1993) diluted 1:5; and rat anti-mCD8α diluted 1:100 (Caltag). FITC-, Cy3-, or Cy5-conjugated secondary antibodies (Jackson ImmunoResearch) were used at a dilution of 1:400.

Acknowledgments

Appendix A. Supplementary data

Supplementary data associated with this article can be found, in the online version, at doi:10.1016/j.mcn.2008.01.015.

References

Aricescu, A.R., McKinnell, I.W., Halfter, W., Stoker, A.W., 2002. Heparan sulfate proteoglycans are ligands for receptor protein tyrosine phosphatase sigma. Mol. Cell. Biol. 22, 1881–1892.

Babu, K., Bahri, S., Alphey, L., Chia, W., 2005. Bifocal and PP1 interaction regulates targeting of the R-cell growth cone in *Drosophila*. Dev. Biol. 288, 372–386.

Babu, K., Cai, Y., Bahri, S., Yang, X., Chia, W., 2004. Roles of Bifocal, Homer, and F-actin in anchoring Oskar to the posterior cortex of *Drosophila* oocytes. Genes Dev. 18, 138–143.

Bahri, S.M., Yang, X., Chia, W., 1997. The *Drosophila* bifocal gene encodes a novel protein which colocalizes with actin and is necessary for photoreceptor morphogenesis. Mol. Cell. Biol. 17, 5521–5529.

Clandinin, T.R., Lee, C.H., Herman, T., Lee, R.C., Yang, A.Y., Ovasapyan, S., Zipursky, S.L., 2001. *Drosophila* LAR regulates R1-R6 and R7 target specificity in the visual system. Neuron 32, 237–248.

Crittenden, J.R., Skoulakis, E.M., Han, K.A., Kalderon, D., Davis, R.L., 1998. Tripartite mushroom body architecture revealed by antigenic markers. Learn. Mem. (Cold Spring Harbor, N.Y) 5, 38–51.

Desai, C., Purdy, J., 2003. The neural receptor protein tyrosine phosphatase DPTP69D is required during periods of axon outgrowth in *Drosophila*. Genetics 164, 575–588.

Desai, C.J., Gindhart Jr., J.G., Goldstein, L.S., Zinn, K., 1996. Receptor tyrosine phosphatases are required for motor axon guidance in the *Drosophila* embryo. Cell 84, 599–609.

Desai, C.J., Krueger, N.X., Saito, H., Zinn, K., 1997. Competition and cooperation among receptor tyrosine phosphatases control motoneuron growth cone guidance in *Drosophila*. Development (Cambridge, England) 124, 1941–1952.

Desai, C.J., Popova, E., Zinn, K., 1994. A *Drosophila* receptor tyrosine phosphatase expressed in the embryonic CNS and larval optic lobes is a member of the set of proteins bearing the "HRP" carbohydrate epitope. J. Neurosci. 14, 7272–7283.

Dietzl, G., Chen, D., Schnorrer, F., Su, K.C., Barinova, Y., Fellner, M., Gasser, B., Kinsey, K., Oppel, S., Scheiblauer, S., Couto, A., Marra, V., Keleman, K., Dickson, B.J., 2007. A genome-wide transgenic RNAi library for conditional gene inactivation in *Drosophila*. Nature 448, 151–156.

Fahrbach, S.E., 2006. Structure of the mushroom bodies of the insect brain. Annu. Rev. Entomol. 51, 209–232.

Flint, A.J., Tiganis, T., Barford, D., Tonks, N.K., 1997. Development of "substrate-trapping" mutants to identify physiological substrates of protein tyrosine phosphatases. Proc. Natl. Acad. Sci. U. S. A. 94, 1680–1685.

Fox, A.N., Zinn, K., 2005. The heparan sulfate proteoglycan syndecan is an in vivo ligand for the *Drosophila* LAR receptor tyrosine phosphatase. Curr. Biol. 15, 1701–1711.

Garrity, P.A., Lee, C.H., Salecker, I., Robertson, H.C., Desai, C.J., Zinn, K., Zipursky, S.L., 1999. Retinal axon target selection in *Drosophila* is regulated by a receptor protein tyrosine phosphatase. Neuron 22, 707–717.

Hamilton, B.A., Ho, A., Zinn, K., 1995. Targeted mutagenesis and genetic analysis of a *Drosophila* receptor-linked protein tyrosine phosphatase gene. Roux's Arch. Dev. Biol. 204, 187–192.

Heisenberg, M., 2003. Mushroom body memoir: from maps to models. Nat. Rev. 4, 266–275.

Ito, K., Awano, W., Suzuki, K., Hiromi, Y., Yamamoto, D., 1997. The *Drosophila* mushroom body is a quadruple structure of clonal units each of which contains a virtually identical set of neurones and glial cells. Development (Cambridge, England) 124, 761–771.

Johnson, K.G., Tenney, A.P., Ghose, A., Duckworth, A.M., Higashi, M.E., Parfitt, K., Marcu, O., Heslip, T.R., Marsh, J.L., Schwarz, T.L., Flanagan, J.G., Van Vactor, D., 2006. The HSPGs Syndecan and Dallylike bind the receptor phosphatase LAR and exert distinct effects on synaptic development. Neuron 49, 517–531.

Johnson, K.G., Van Vactor, D., 2003. Receptor protein tyrosine phosphatases in nervous system development. Physiol. Rev. 83, 1–24.

Kaufmann, N., DeProto, J., Ranjan, R., Wan, H., Van Vactor, D., 2002. *Drosophila* liprin-alpha and the receptor phosphatase Dlar control synapse morphogenesis. Neuron 34, 27–38.

Kidd, T., Bland, K.S., Goodman, C.S., 1999. Slit is the midline repellent for the robo receptor in *Drosophila*. Cell 96, 785–794.

Kobayashi, M., Michaut, L., Ino, A., Honjo, K., Nakajima, T., Maruyama, Y., Mochizuki, H., Ando, M., Ghangrekar, I., Takahashi, K., Saigo, K., Ueda, R., Gehring, W.J., Furukubo-Tokunaga, K., 2006. Differential microarray analysis of *Drosophila* mushroom body transcripts using chemical ablation. Proc. Natl. Acad. Sci. U. S. A. 103, 14417–14422.

Krueger, N.X., Van Vactor, D., Wan, H.I., Gelbart, W.M., Goodman, C.S., Saito, H., 1996. The transmembrane tyrosine phosphatase DLAR controls motor axon guidance in *Drosophila*. Cell 84, 611–622.

Kurusu, M., Awasaki, T., Masuda-Nakagawa, L.M., Kawauchi, H., Ito, K., Furukubo-Tokunaga, K., 2002. Embryonic and larval development of the *Drosophila* mushroom bodies: concentric layer subdivisions and the role of fasciclin II. Development (Cambridge, England) 129, 409–419.

Lee, T., Lee, A., Luo, L., 1999. Development of the *Drosophila* mushroom bodies: sequential generation of three distinct types of neurons from a neuroblast. Development (Cambridge, England) 126, 4065–4076.

Lee, T., Luo, L., 1999. Mosaic analysis with a repressible cell marker for studies of gene function in neuronal morphogenesis. Neuron 22, 451–461.

Lin, H.H., Lai, J.S., Chin, A.L., Chen, Y.C., Chiang, A.S., 2007. A map of olfactory representation in the *Drosophila* mushroom body. Cell 128, 1205–1217.

Masuda-Nakagawa, L.M., Tanaka, N.K., O'Kane, C.J., 2005. Stereotypic and random patterns of connectivity in the larval mushroom body calyx of *Drosophila*. Proc. Natl. Acad. Sci. U. S. A. 102, 19027–19032.

Maurel-Zaffran, C., Suzuki, T., Gahmon, G., Treisman, J.E., Dickson, B.J., 2001. Cell-autonomous and -nonautonomous functions of LAR in R7 photoreceptor axon targeting. Neuron 32, 225–235.

McBride, S.M., Choi, C.H., Wang, Y., Liebelt, D., Braunstein, E., Ferreiro, D., Sehgal, A., Siwicki, K.K., Dockendorff, T.C., Nguyen, H.T., McDonald, T.V., Jongens, T.A., 2005. Pharmacological rescue of synaptic plasticity, courtship behavior, and mushroom body defects in a *Drosophila* model of fragile X syndrome. Neuron 45, 753–764.

Michel, C.I., Kraft, R., Restifo, L.L., 2004. Defective neuronal development in the mushroom bodies of *Drosophila* fragile X mental retardation 1 mutants. J. Neurosci. 24, 5798–5809.

Moreau-Fauvarque, C., Taillebourg, E., Boissoneau, E., Mesnard, J., Dura, J.M., 1998. The receptor tyrosine kinase gene linotte is required for neuronal pathway selection in the *Drosophila* mushroom bodies. Mech. Dev. 78, 47–61.

Newsome, T.P., Asling, B., Dickson, B.J., 2000. Analysis of *Drosophila* photoreceptor axon guidance in eye-specific mosaics. Development (Cambridge, England) 127, 851–860.

Nicolas, E., Preat, T., 2005. *Drosophila* central brain formation requires Robo proteins. Dev. Genes Evol. 215, 530–536.

Nishiyama, M., Hoshino, A., Tsai, L., Henley, J.R., Goshima, Y., Tessier-Lavigne, M., Poo, M.M., Hong, K., 2003. Cyclic AMP/GMP-dependent modulation of Ca2+ channels sets the polarity of nerve growth-cone turning. Nature 423, 990–995.

Pan, L., Zhang, Y.Q., Woodruff, E., Broadie, K., 2004. The *Drosophila* fragile X gene negatively regulates neuronal elaboration and synaptic differentiation. Curr. Biol. 14, 1863–1870.

Pascual, A., Preat, T., 2001. Localization of long-term memory within the *Drosophila* mushroom body. Science (New York, N.Y 294, 1115–1117.

Qian, M., Pan, G., Sun, L., Feng, C., Xie, Z., Tully, T., Zhong, Y., 2007. Receptor-like tyrosine phosphatase PTP10D is required for long-term memory in *Drosophila*. J. Neurosci. 27, 4396–4402.

Ruan, W., Long, H., Vuong, D.H., Rao, Y., 2002. Bifocal is a downstream target of the Ste20-like serine/threonine kinase misshapen in regulating photoreceptor growth cone targeting in *Drosophila*. Neuron 36, 831–842.

Schindelholz, B., Knirr, M., Warrior, R., Zinn, K., 2001. Regulation of CNS and motor axon guidance in *Drosophila* by the receptor tyrosine phosphatase DPTP52F. Development (Cambridge, England) 128, 4371–4382.

Schmucker, D., Clemens, J.C., Shu, H., Worby, C.A., Xiao, J., Muda, M., Dixon, J.E., Zipursky, S.L., 2000. *Drosophila* Dscam is an axon guidance receptor exhibiting extraordinary molecular diversity. Cell 101, 671–684.

Strausfeld, N.J., Hansen, L., Li, Y., Gomez, R.S., Ito, K., 1998. Evolution, discovery, and interpretations of arthropod mushroom bodies. Learn. Mem. (Cold Spring Harbor, N.Y 5, 11–37.

Strausfeld, N.J., Sinakevitch, I., Vilinsky, I., 2003. The mushroom bodies of *Drosophila melanogaster*: an immunocytological and golgi study of Kenyon cell organization in the calyces and lobes. Microsc. Res. Tech. 62, 151–169.

Sun, Q., Bahri, S., Schmid, A., Chia, W., Zinn, K., 2000. Receptor tyrosine phosphatases regulate axon guidance across the midline of the *Drosophila* embryo. Development (Cambridge, England) 127, 801–812.

Sun, Q., Schindelholz, B., Knirr, M., Schmid, A., Zinn, K., 2001. Complex genetic interactions among four receptor tyrosine phosphatases regulate axon guidance in *Drosophila*. Mol. Cell. Neurosci. 17, 274–291.

Tian, S.S., Tsoulfas, P., Zinn, K., 1991. Three receptor-linked protein-tyrosine phosphatases are selectively expressed on central nervous system axons in the *Drosophila* embryo. Cell 67, 675–685.

Vactor, D.V., Sink, H., Fambrough, D., Tsoo, R., Goodman, C.S., 1993. Genes that control neuromuscular specificity in *Drosophila*. Cell 73, 1137–1153.

Wojtowicz, W.M., Flanagan, J.J., Millard, S.S., Zipursky, S.L., Clemens, J.C., 2004. Alternative splicing of *Drosophila* Dscam generates axon guidance receptors that exhibit isoform-specific homophilic binding. Cell 118, 619–633.

Yang, X.H., Seow, K.T., Bahri, S.M., Oon, S.H., Chia, W., 1991. Two *Drosophila* receptor-like tyrosine phosphatase genes are expressed in a subset of developing axons and pioneer neurons in the embryonic CNS. Cell 67, 661–673.

Yoshikawa, S., McKinnon, R.D., Kokel, M., Thomas, J.B., 2003. Wnt-mediated axon guidance via the *Drosophila* Derailed receptor. Nature 422, 583–588.

Zars, T., Fischer, M., Schulz, R., Heisenberg, M., 2000. Localization of a short-term memory in *Drosophila*. Science (New York, N.Y) 288, 672–675.

Zhan, X.L., Clemens, J.C., Neves, G., Hattori, D., Flanagan, J.J., Hummel, T., Vasconcelos, M.L., Chess, A., Zipursky, S.L., 2004. Analysis of Dscam diversity in regulating axon guidance in *Drosophila* mushroom bodies. Neuron 43, 673–686.

Zhu, S., Chiang, A.S., Lee, T., 2003. Development of the *Drosophila* mushroom bodies: elaboration, remodeling and spatial organization of dendrites in the calyx. Development (Cambridge, England) 130, 2603–2610.